First look at RNA in L-configuration

M. Vallazza,[a]‡ M. Perbandt,[b]‡ S. Klussmann,[c] W. Rypniewski,[b] H. M. Einspahr,[d] V. A. Erdmann[a] and Ch. Betzel[b]*

[a]Institutes of Biology, Chemistry and Pharmacy, Free University of Berlin, Biochemistry: Thielallee 63, 14195 Berlin, Germany, [b]Universitätsklinikum Hamburg-Eppendorf, Zentrum für Experimentelle Medizin, Institut für Biochemie und Molekularbiologie I, Zelluläre Signaltransduktion, c/o DESY Building 22a, Notkestrasse 85, 22603 Hamburg, Germany, [c]NOXXON Pharma AG, Max-Dorn-Strasse 8-10, 10589 Berlin, Germany, [d]Institute of Bioorganic Chemistry, Polish Academy of Sciences, Noskowskiego 12/14, 61-7004 Poznan, Poland, and [e]PO Box 6395, Lawrenceville, New Jersey 08648-0395, USA

‡ These authors contributed equally to this work.

Correspondence e-mail: betzel@unisgi1.desy.de

Nucleic acid molecules in the mirror image or L-configuration are unknown in nature and are extraordinarily resistant to biological degradation. The identification of functional L-oligonucleotides called Spiegelmers offers a novel approach for drug discovery based on RNA. The sequence r(CUGGGCGG)·r(CCGCCUGG) was chosen as a model system for structural analysis of helices in the L-configuration as the structure of the D-form of this sequence has previously been determined in structural studies of 5S RNA domains, in particular domain E of the *Thermus flavus* 5S rRNA [Perbandt *et al.* (2001), *Acta Cryst.* D**57**, 219–224]. Unexpectedly, the results of crystallization trials showed little similarity between the D- and the L-forms of the duplex in either the crystallization hits or the diffraction performance. The crystal structure of this L-RNA duplex has been determined at 1.9 Å resolution with R_{work} and R_{free} of 23.8 and 28.6%, respectively. The crystals belong to space group $R32$, with unit-cell parameters $a = 45.7$, $c = 264.6$ Å. Although there are two molecules in the asymmetric unit rather than one, the structure of the L-form arranges helical pairs in a head-to-tail fashion to form pseudo-continuous infinite helices in the crystal as in the D-form. On the other hand, the wobble-like G·C$^+$ base pair seen in the D-RNA analogue does not appear in the L-RNA duplex, which forms a regular double-helical structure with typical Watson–Crick base pairing.

1. Introduction

The diverse functions of ribonucleic acids as information carriers (mRNA), adapters (tRNA) or scaffolds and catalysts (rRNA) reflect the crucial importance of RNA within the living cell and its significance as essential for life itself. A number of novel properties of RNA molecules make them useful in new applications in biotechnology and molecular medicine (Erdmann & Fuerste, 1999; Sullenger & Gilboa, 2002). Three examples are noted here. Firstly, the discovery of self-cleaving RNA and natural ribozymes and the development of new catalytic RNA molecules not only support the hypothesis of an early RNA world, but also open up new opportunities for novel clinical applications (Kruger *et al.*, 1982; Seelig & Jäschke, 1999; Ban *et al.*, 2000; Johnston *et al.*, 2001). Secondly, RNA molecules have also been found to express high affinity for a wide variety of target molecules. Called aptamers (Ellington & Szostak, 1990), these RNA ligands can be produced by an efficient *in vitro* selection procedure (Tuerk & Gold, 1990). Because of their high affinity for a broad spectrum of structural targets, such RNA molecules have properties comparable to antibodies. L-RNA versions of these molecules, called Spiegelmers, are especially long-lived as they are essentially impervious to natural degradation processes. Thirdly, a number of small RNA

molecules have been found to interfere with and regulate gene expression. The action of RNA interference on dsRNA to trigger sequence-specific gene silencing is likely to find future application in novel therapeutics against a variety of diseases (Hannon, 2002; Gruenweller *et al.*, 2003).

These and other structural and functional properties of RNA are being employed in the rapidly evolving area of RNA technology and, as a consequence, have intensified and underscored a great need for more structural understanding of folding motifs in order to design functional RNA molecules. So far, only about 670 structures of RNA molecules have been determined, 400 of them by X-ray crystallography and about 270 by NMR techniques; by comparison, some 1300 DNA structures and nearly 23 500 protein structures have been characterized [according to the Nucleic Acid Data Bank (NDB) and the Protein Data Bank (PDB)].

In order to initiate studies of the structural features of mirror-reflected RNA motifs, we have synthesized and crystallized a Spiegelmer. Spiegelmers are being developed to bind pharmacologically interesting targets with high affinity and specificity. In terms of biophysical behaviour, Spiegelmers are comparable to high-affinity aptamers, which are D-oligonucleotides. With respect to nucleolytic degradation, however, Spiegelmers are much more biostable than aptamers (Klussmann *et al.*, 1996), since neither Spiegelmers nor the corresponding RNases are found in nature. By exploiting chirality, Spiegelmers represent a promising approach in RNA drug stabilization that is additive to other approaches such as chemical modification using phosphorothioates or locked nucleic acids (Kurreck *et al.*, 2002; Gruenweller *et al.*, 2003).

Spiegelmers were originally developed in our laboratory (Klussmann *et al.*, 1996; Nolte *et al.*, 1996). In order to design a Spiegelmer, a D-RNA aptamer is first selected to bind the unnatural enantiomeric form of a target by means of the *in vitro* selection procedure mentioned above (Tuerk & Gold, 1990). In the second step, the Spiegelmer, the mirror-image analogue of the aptamer, is chemically synthesized. This Spiegelmer specifically recognizes the natural enantiomeric form of the target. Spiegelmers specifically binding targets such as the gonadotropin-releasing hormone (GnRH), nociceptin and the α-calcitonin gene-related peptide (αCGRP) are among those currently being developed in the pharmaceutical industry (Leva *et al.*, 2002; Wlotzka *et al.*, 2002). αCGRP is a potent endogenous vasodilator that may be implicated in the genesis of migraine attacks. Intercepting and inactivating αCGRP by means of a Spiegelmer will offer a new strategy for treating this class of headaches (Hakala & Vihinen, 1994).

In order to understand and realise the potential of the Spiegelmer strategy, it is important to recognize and appreciate those sequence-specific mechanisms that govern not only the intermolecular interactions between L-RNA and target, but also the role of solvent in the mediation of intermolecular contacts and the intramolecular interactions responsible for RNA folding and function. In this context, we are particularly interested in water arrangements within these structures. The important role of hydration in RNA assembly has been recognized (Barciszewski *et al.*, 1999) and a highly structured network of hydrogen bonds has a principal role in maintaining the tertiary structures of RNA (Betzel *et al.*, 1994).

To date, no structure of an L-RNA fragment, either Spiegelmer or racemate, has been reported. In this paper, we compare the structure of a previously determined D-RNA duplex at 1.6 Å resolution (Perbandt *et al.*, 2001) to that of its L-RNA analogue at 1.9 Å resolution. This latter is the first structure of an L-RNA oligomer. The comparison shows a surprising divergence between the enantiomers in the results of crystallization trials and in the structures and hydration patterns.

2. Material and methods

2.1. Synthesis and crystallization

The L-RNA sequences E3-79 (5′-CUGGGCGG-3′) and E3-90 (5′-CCGCCUGG-3′) were synthesized by the use of phosphoramidite chemistry and were purified as previously described (Wlotzka *et al.*, 2002). The determination of concentrations by use of the Lambert–Beer equation and the annealing of the L-oligoribonucleotides were performed with reference to Vallazza *et al.* (2001). Because of the expected equivalence of the enantiomers, we applied the known specific extinction coefficients for the D-RNA analogue ($\varepsilon_{E3-79} = 62\ 167\ l\ mol^{-1}\ cm^{-1}$ and $\varepsilon_{E3-90} = 60\ 171\ l\ mol^{-1}\ cm^{-1}$) in calculations for the Spiegelmer. The initial crystallization trials replicated the optimized conditions for the previously published D-RNA analogue (Vallazza *et al.*, 2001, 2002). This was a hanging-drop vapor-diffusion experiment equilibrating 2 µl drops [half reservoir solution containing 10%(v/v) 2-methyl-2,4-pentanediol (MPD), 80 mM KCl, 20 mM BaCl$_2$, 12 mM spermine tetrahydrochloride (SpCl$_4$), 40 mM sodium cacodylate pH 6.0 and half 0.25 mM RNA in double-distilled water] against 0.8 ml reservoir solution with 30%(v/v) MPD. Unexpectedly, these conditions failed to yield crystals of the L-RNA enantiomer. Subsequently, application of 216 commercial screening protocols [Nucleic Acid Mini (NUC) Screens, Crystal Screen 1 and Crystal Screen 2, Grid Screen Ammonium Sulfate and Natrix (Nos. 25–48) from Hampton Research; JBScreen 6 from JenaBioscience; RNA–MPD Screen (Nos. 25–48) from Vallazza *et al.* (2001)] at 291 K produced hits that led to the crystals used in this study.

Attempts to optimize crystal growth also included experiments in microgravity, as there is evidence that growth in microgravity can narrow mosaic spreads in protein and RNA crystals (Snell *et al.*, 1995; Borgstahl *et al.*, 2001). Nine crystallization trials were performed on the International Space Station (ISS) in the High Density Protein Crystal Growth (HDPCG) apparatus (previously described by Vallazza *et al.*, 2002) during the mission ISS-8A for a period of 67 d from 10 April to 17 June 2002. These trials tested four conditions: (i) NUC No. 8, (ii) NUC No. 15, (iii) Crystal Screen Cryo No. 15 and (iv) Crystal Screen No. 39.

The best crystal so far, which was used for data collection to 1.9 Å resolution and is shown in Fig. 1, was a rod-shaped
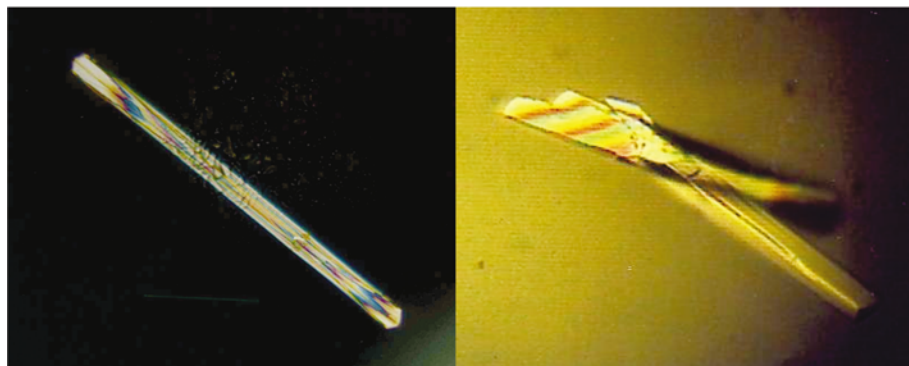
Figure 1
Crystals of D-RNA (left) and Spiegelmer (right). The D-RNA crystal has dimensions of $0.05 \times 0.05 \times 0.8$ mm and the crystal of the Spiegelmer has approximate dimensions $0.07 \times 0.07 \times 0.67$ mm.

Table 1
Data-collection and refinement statistics.

Data for the outer resolution shell, 1.95–1.9 Å, are included in parentheses.

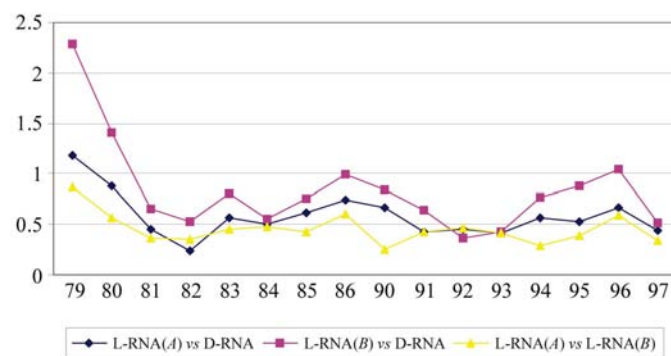|	
Space group	$R32$
Unit-cell parameters (Å)	
$\quad a = b$	45.7
$\quad c$	264.6
Matthews coefficient (Å^3 Da^{-1})	2.7
Solvent content (%)	64.0
Mosaicity (°)	1.2
Resolution range (Å)	20–1.9
No. of unique reflections	8949 (511)
R_{sym} (final shell)	0.064 (0.470)
Completeness (%)	98.7 (98.9)
R factor (final shell)	0.238 (0.292)
R_{free}	0.286 (0.413)
No. of atoms	
$\quad$ Nucleic acid atoms	676
$\quad$ Water O atoms	129

Figure 2
Graph showing the r.m.s. deviation between individual strands of the L-RNA *versus* D-RNA and between the two L-RNA molecules in the asymmetric unit. The labeling of the strands is according to the reference segment of helix E of 5S RNA (Perbandt *et al.*, 2001): I, 79–86; II, 90–97.

specimen from trials grown at 291 K in the laboratory at unit gravity by equilibration of a 2 μl drop of 0.125 mM L-RNA in 0.05 M Na HEPES pH 7.5, 1%(v/v) PEG 400, 1 M (NH$_4$)$_2$SO$_4$ against a reservoir of 0.8 ml having twice the concentration of all components but without RNA. The crystal was cryo-

protected with 15%(v/v) glycerol in 0.085 M Na HEPES pH 7.5, 1.7%(v/v) PEG 400 and 1.7 M (NH$_4$)$_2$SO$_4$.

2.2. Data collection

Diffraction data were collected at 100 K using synchrotron radiation (Consortium Beamline X13, DESY, Germany). The data were indexed and integrated with the program *DENZO* (Otwinowski & Minor, 1997). The space group was assigned as rhombohedral *R*32, with two duplexes in the asymmetric unit. The data-collection statistics are summarized in Table 1. This space group is the same as that found for the D-RNA form and the unit-cell parameters are homologous, with the single exception that c is doubled, so that the L-form has two molecules in the asymmetric unit.

2.3. Structure solution and refinement

The structure was solved by molecular-replacement methods applying the program package *AMoRe* (Navaza, 1994). The coordinates of the D-RNA form of the duplex r(CUGGGCGG)·r(CCGCCUGG), which corresponds to helix E of 5S rRNA (Perbandt *et al.*, 2001), were transformed into the L-form by reflection across the x axis. A rotation–translation solution was obtained for two molecules in the asymmetric unit based on this coordinate set as the search model. For refinement, the program *REFMAC* (Collaborative Computational Project, Number 4, 1994) was applied with a subset of reflections (5%) set aside for R_{free} calculations (Brünger, 1992). No restraints were applied to the chirality. Rigid-body refinement of the initial solution reduced the R factor to 35.2% and R_{free} to 37.3% for all data in the resolution range 10.0–3.0 Å. A few cycles of restrained refinement reduced the R and R_{free} values further to 27.1 and 31.9%, respectively. 127 water molecules were located as peaks above 3σ in a $F_o - F_c$ difference map with corresponding peaks above 1σ in a $2F_o - F_c$ density map. For regions of particular interest, omit maps were calculated to verify the structure with reduced bias. The cycles of individual isotropic B-factor refinement that followed reduced the R value to 23.8% and R_{free} to 28.6% for all data in the resolution range 20.0–1.9 Å. The structure is well ordered throughout as shown in Fig. 2. The refinement statistics are summarized in Table 1.

3. Results and discussion

3.1. Crystallization

Our first crystallization trials attempted to screen conditions close to those optimized for the D-RNA analogue. That this screen failed came as something of a surprise to us. The results of the commercial screen-based trials that followed are shown in Table 2, where they are compared with results for the D-RNA analogue. Well shaped crystals were found in 21 of the

Table 2
Crystallization conditions and crystal features of the Spiegelmer and its D-RNA.

Abbreviations: AS, ammonium sulfate; MPD, 2-methyl-2,4-pentanediol; NUC, Nucleic Acid Mini Screen; SpCl$_4$, spermine tetrahydrochloride.

Screen, No.	Precipitant	Salt	Buffer	pH	Polyamine	Crystal features Spiegelmer	D-RNA
Crystal, 15	30%(w/v) PEG 8000	200 mM AS	100 mM Na cacodylate	6.5	None	No diffraction	No crystals
Crystal, 17	30%(w/v) PEG 4000	200 mM Li$_2$SO$_4$	100 mM Tris–HCl	8.5	None	No diffraction	No crystals
Crystal, 32	2.0 M AS	None	None	—	None	2.0 Å, twinned	Too small
Crystal, 39	2.0 M AS/2%(v/v) PEG 400	None	100 mM Na HEPES	7.5	None	1.9 Å	No crystals
Crystal 2, 25	1.8 M AS	10 mM CoCl$_2$	100 mM Na MES	6.5	None	No diffraction	No crystals
Crystal 2, 26	30%(w/v) PEG 5000 MME	200 mM AS	100 mM Na MES	6.5	None	No diffraction	No crystals
JBScreen 6, 1	0.5 M AS	1 M Li$_2$SO$_4$	100 mM Na citrate	6.2	None	No diffraction	Split
JBScreen 6, 12	1.8 M AS	None	100 mM Na MES	6.5	None	No diffraction	No diffraction
JBScreen 6, 13	2.0 M AS	2 M NaCl	None		None	No diffraction	No crystals
JBScreen 6, 14	2.0 M AS	None	100 mM Na acetate	4.6	None	No diffraction	No crystals
Natrix, 30	1.6 M AS	10 mM MgCl$_2$	50 mM Na HEPES	7.0	None	Split	Split
Natrix, 40	1.6 M AS	10 mM MgCl$_2$	50 mM Tris–HCl	7.5	None	Split	No crystals
Natrix, 46	35%(w/v) hexanediol	5 mM MgSO$_4$	50 mM Tris–HCl	8.5	None	No diffraction	No crystals
Natrix, 47	30%(v/v) PEG 400	100/10 mM KCl/MgCl$_2$	50 mM Tris–HCl	8.5	None	No diffraction	No crystals
NUC, 8	10%(v/v) MPD	80 mM NaCl	40 mM Na cacodylate	6.0	12 mM SpCl$_4$	1.7 Å, mosaic	Too small
NUC, 10	10%(v/v) MPD	12/80 mM NaCl/KCl	40 mM Na cacodylate	6.0	12 mM SpCl$_4$	1.6 Å, mosaic	Split
NUC, 15	10%(v/v) MPD	80 mM KCl	40 mM Na cacodylate	7.0	12 mM SpCl$_4$	1.8 Å, twinned	1.9 Å
NUC, 17	10%(v/v) MPD	80 mM NaCl	40 mM Na cacodylate	7.0	12 mM SpCl$_4$	2.0 Å, twinned	Too small
RNA–MPD, 29	10%(v/v) MPD	80 mM NaCl	40 mM Na cacodylate	7.2	100 mM SpCl$_4$	Split	Split
RNA–MPD, 33	10%(v/v) MPD	200 mM KCl	40 mM Na cacodylate	6.0	12 mM SpCl$_4$	Split	No diffraction
RNA–MPD, 43	10%(v/v) MPD	40/80 mM LiCl/SrCl$_2$	40 mM Na cacodylate	6.0	12 mM SpCl$_4$	Split	No crystals

Table 3
Helical parameters.

(a) Overall helical parameters.

	Twist (°)	Rise (Å)	Roll (°)	X-Disp. (Å)	Prop. (°)
L-RNA 8 bp (molecule A)	−32.2	2.71	5.4	−5.4	−9.6
L-RNA 8 bp (molecule B)	−31.6	2.75	5.1	−5.6	−8.2
D-RNA 8 bp	32.9	2.57	6.7	−5.3	−10.8
[U(UA)$_6$]$_2$	32.2	2.78	9.4	−3.6	−19.1
tRNA	33.2	2.50	5.2	−4.4	−14.2

(b) Local helical parameters for L-RNA and its corresponding D-RNA.

	Twist (°)			Rise (Å)			X-Disp. (Å)		
	L-RNA A	L-RNA B	D-RNA	L-RNA A	L-RNA B	D-RNA	L-RNA A	L-RNA B	D-RNA
C·G									
	−30.03	−28.01	31.38	3.13	3.38	3.20	−4.74	−5.11	−3.77
U·G									
	−38.48	−39.17	43.48	1.80	1.82	1.89	−7.90	−8.27	−5.45
G·U									
	−28.18	−25.92	29.90	2.99	2.95	2.87	−5.53	−6.05	−5.36
G·C									
	−32.53	−32.93	29.39	2.38	2.56	2.41	−6.07	−5.67	−6.84
G·C									
	−29.55	−29.19	28.10	3.30	3.29	3.16	−1.65	−1.70	−3.40
C·G									
	−34.53	−33.03	35.24	2.27	2.38	1.72	−7.99	−7.76	−7.60
G·C									
	−31.56	−32.81	33.02	3.14	2.89	2.74	−4.22	−4.78	−4.77
G·C									

trials with L-RNA. Although ten of these conditions gave crystals for both enantiomers, the D-RNA and the Spiegelmer crystals at each condition differed sharply in size, shape and diffraction quality (Table 2).

In our experience, the primary challenge to structure studies of these RNA molecules has always been to find a crystal specimen with a mosaic spread narrow enough to permit useful data collection. Many samples must be tried and discarded before a satisfactory one is found. Because of this, for our work on the D-RNA duplex we also tried crystallization under microgravity conditions to good effect in that the results included more crystals with improved size and useful mosaic spread that gave data of improved quality when compared with samples grown in gravity (Lorenz et al., 2000; Vallazza et al., 2002).

Because of similar problems, microgravity crystallization was also tried with the Spiegelmer and similar improvements were obtained. Five of the nine crystallization trials performed in microgravity experiments produced crystals and approximately 75% had useful mosaicities and displayed enhanced resolution to about 2.0 Å over that obtained in ground-based controls. However, in this case the crystal used for data collection, which scattered up to 1.9 Å resolution, was grown in the home laboratory at terrestrial gravity. It was also obtained by precipitation with ammonium sulfate, not MPD (see §2).

3.2. Structural features

The L-RNA duplex adopts a standard A-form conformation with all the helical parameters resembling those of a piece of

A-RNA, as summarized in Table 3. Considering that 11 residues are required per helical turn, the average helical twist of the octamer duplex is 32.2° for molecule A and 31.6° for molecule B. The average rise per residue of 2.71 and 2.75 Å for A and B, respectively, is approximately 5% higher than found for the D-form (average 2.6 Å) and is at the high end of the range shown by D-RNA forms; it is exceeded only by that of the $[U(UA)_6]_2$ (Dock-Bregon et al., 1989) duplex. In contrast, the roll of 5.2 and 5.1°, respectively, is at the low end of the D-RNA range and is close to that of tRNA. Finally, the average propeller twist of the Spiegelmer duplex, −9.6 and −8.2° for A and B, respectively, is lower than the range shown in D-RNA structures, but closest to that of its D-RNA

analogue. All of the ribose rings of the present structure are either in C3′-exo or 2′-endo-3′-exo puckering conformations and all α torsion angles are in the g^+ conformation and correlated with the γ torsion angles, which are in the g^- conformation (Tables 3a and 3b). The P—P interstrand distances have mean values, considering both molecules in the asymmetric unit, of 5.92 (32) and 5.85 (20) Å for strands I and II, respectively. The D-form has values of 5.86 (23) and 5.80 (22) Å.

When the D-RNA duplex structure r(CUGGGCGG)·r(CCGCCUGG) is transformed by mirror operation to a left-handed L-RNA model and superimposed on the structures of Spiegelmer duplexes A and B, the r.m.s. deviations between the transformed model and the structure are 0.57 and 0.85 Å, respectively, as also shown in Fig. 2. In each comparison, it is the terminal residues that give the highest r.m.s. deviations, suggesting that the differences arise from flexibility in the terminal residue conformations. The structures of A and B are very similar, differing by an r.m.s. deviation of 0.46 Å (Fig. 2).

There is no irregular hydrogen bonding between base pairs in either of the two independent helices in this structure and no departures from a regular Watson–Crick base-pair formation (Fig. 3a). This contrasts with the results for the D-RNA structure, which features an unusual G92·C84 base pairing in a wobble-like conformation (Fig. 3b). A contributing factor to the removal of this unusual base-pair configuration may be the shift in pH from 6.0 in the crystallization buffer of the D-RNA to 7.5 in that of the Spiegelmer, a shift that may prevent the protonation of the N3 atom of the cytosine.

The two G·U pairings are in tandem wobble conformation with the purines, forming the so-called 'cross-strand G stack' (Perbandt et al., 2001). The solvent content is similar and the number of water molecules located is almost identical to that of the D-form structure, taking into account the doubling of the c axis in the L-form. 127 independent solvent molecules were identified in the Spiegelmer structure, 45 of which were found in the major grooves of the RNA helices. The internal water molecules are shown in Fig. 4, using a space-filling representation to demonstrate the thorough filling of the interior helix, with almost bulk solvent in the narrow minor and the deep major grooves. At the end of the helical segments, more regular water networks stabilize the duplexes. A superposition of the water structures of the two unique
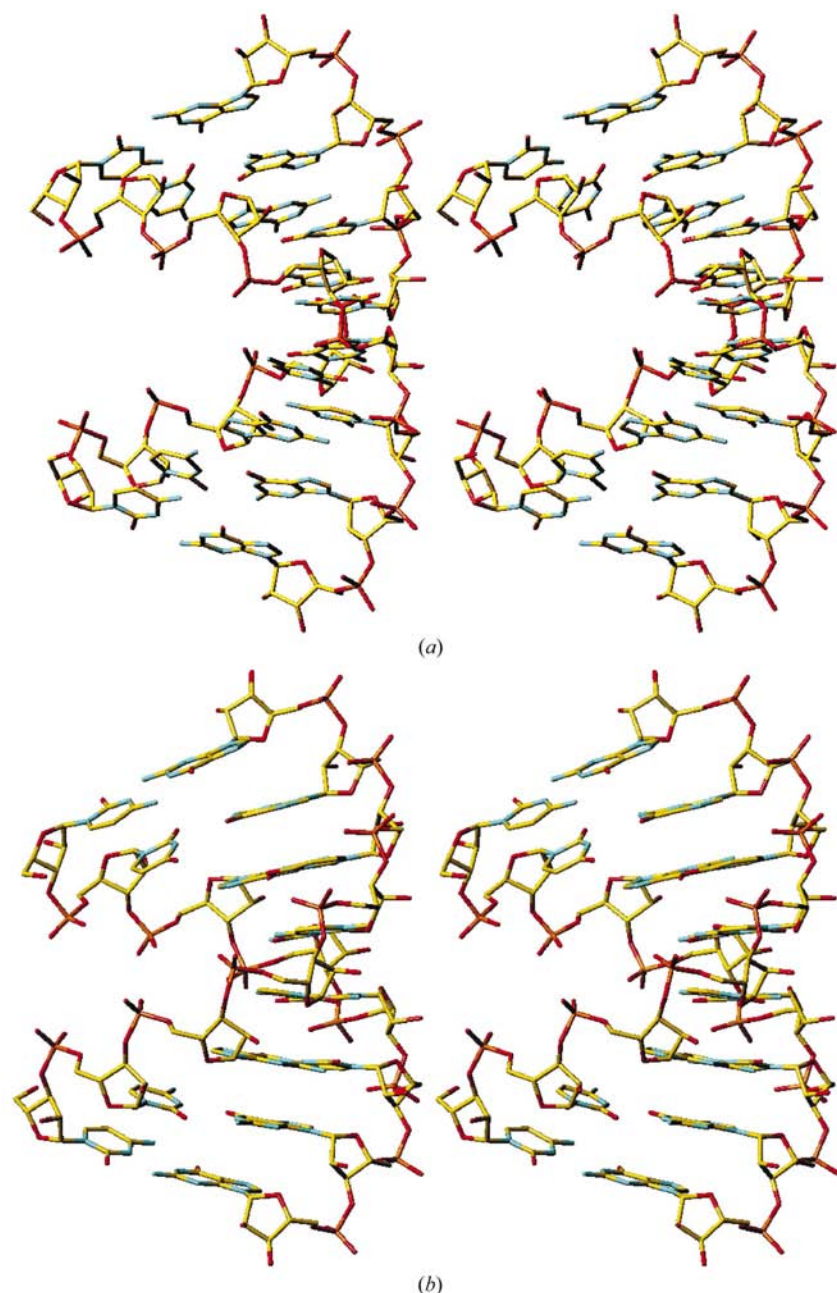

Figure 3
(a) Stereoview of the D-RNA 8 bp helix and (b) of the analogue L-RNA 8 bp helix.

molecules in the structure shows only ten solvent molecules superimposing within a distance of 1.0 Å, of which six are internal waters. 35 water molecules superimpose within 1.5 Å, with 12 belonging to internal waters.

4. Conclusions

The emerging applications of mirror-image oligonucleotides led us to structural investigations of this novel RNA class. Although enantiomers should expose identical chemical and physical features to solvent in accordance with symmetry, the two enantiomers required different conditions to produce crystals good enough for diffraction experiments. Similar but not identical results were observed when crystallizing a mirror-imaged protein, D-monellin (Hung *et al.*, 1998). We are not sure what causes these differences in crystallization behaviour. There may be some unrecognized differences in the two starting RNA solutions. The parity-violating energy difference between ribose enantiomers, which theoretically amounts to 10^{-13} J mol^{-1} in favour of the D-RNA enantiomer (Tranter, 1987), hardly seems to be at play. However, the gradient of the free energy to be minimized as the thermodynamic requirement of the crystallization process is increased to a slightly higher level owing to the higher Gibbs energy of the Spiegelmer. That fact might change the crystallization behavior. The clear difference in crystallization hits could serve as an indication that the theoretically predicted effects of parity violation are actually larger than predicted (Berger *et al.*, 2001; Quack, 2002).

The variations in crystallization conditions for the two enantiomers undoubtedly exert important influences on the crystal structures and are therefore responsible for some of the distinguishing features between these Spiegelmer and D-RNA structures. The disappearance of a wobble-like G·C$^+$ base pair and the altered hydration in the Spiegelmer structure are two of the more prominent differences. The obtained differences in the solvent arrangements in the two RNA structures are also likely to be a factor. They may result from differences in ribose chirality. It has been suggested that a chiral water network may represent another factor influencing the structures of enantiomers and their crystal packing (Hung *et al.*, 1998).

In summary, this first structure of a Spiegelmer is a potentially important contribution to the knowledge of the structures of these oligomeric RNAs and will aid in the design of other RNAs for a variety of important uses. Furthermore, the characterization of folding motifs such as the G·C$^+$ base pair and the definition of structural elements involved in target interactions such as the G·U base pairs add essential knowledge for the optimization of these high-affinity binding molecules.
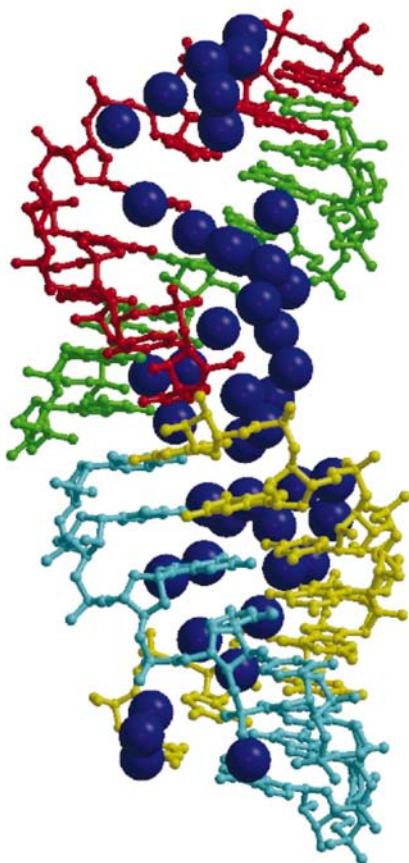
Figure 4
The two L-RNA molecules in the asymmetric unit shown in different colours. The internal waters are represented in blue using their van der Waals radii to indicate the filling of the interior of the helix.

References

Ban, N., Nissen, P., Hansen, J., Moore, P. B. & Steitz, T. A. (2000). *Science*, **289**, 905–920.

Barciszewski, J., Jurczak, J., Porowski, S., Specht, T. & Erdmann, V. A. (1999). *Eur. J. Biochem.* **260**, 293–307.

Berger, R., Quack, M. & Stohner, J. (2001). *Angew. Chem.* **113**, 1716–1719.

Betzel, C., Lorenz, S., Fürste, J. P., Bald, R., Zhang, M., Schneider, T. R., Wilson, K. S. & Erdmann, V. A. (1994). *FEBS Lett.* **351**, 159–164.

Borgstahl, G. E. O., Vahedi-Fardi, A., Lovelace, J., Bellamy, H. & Snell, E. H. (2001). *Acta Cryst.* D**57**, 1204–1207.

Brünger, A. T. (1992). *X-PLOR. Version 3.1. A System for Crystallography and NMR.* New Haven, CT, USA: Yale University Press.

Collaborative Computational Project, Number 4 (1994). *Acta Cryst.* D**50**, 760–763.

Dock-Bregon, A. C., Chevrier, B., Podjarny, A., Johnson, J., deBear, J. S., Gough, G. R., Gilham, P. T. & Moras, D. (1989). *J. Mol. Biol.* **209**, 459–474.

Ellington, A. & Szostak, J. W. (1990). *Nature (London)*, **346**, 818–822.

Erdmann, V. A. & Fuerste, J. P. (1999). *Euro-biotech*, **2000**, 104–108.

Gruenweller, A., Wyszko, E., Bieber, B., Jahnel, R., Erdmann, V. A. & Kurreck, J. (2003). *Nucleic Acids Res.* **31**, 3185–3193.

Hakala, J. M. L. & Vihinen, M. (1994). *Protein Eng.* **7**, 1069–1075.

Hannon, G. J. (2002). *Nature (London)*, **418**, 244–251.

Hung, L. W., Kohmura, M., Ariyoshi, Y. & Kim, S.-H. (1998). *Acta Cryst.* D**54**, 494–500.

Johnston, W. K., Unrau, P. J., Lawrence, M. S., Glasner, M. E. & Bartel, D. P. (2001). *Science*, **292**, 1319–1325.

Klussmann, S., Nolte, A., Bald, R., Erdmann, V. A. & Fuerste, J. P. (1996). *Nature Biotechnol.* **14**, 1112–1115.

Kruger, K., Grabowski, P. J., Zaug, A. J., Sands, J., Gottschling, D. E. & Cech, T. R. (1982). *Cell*, **31**, 147–157.

Kurreck, J., Wyszko, E., Gillen, C. & Erdmann, V. A. (2002). *Nucleic Acids Res.* **30**, 1911–1918.

Leva, S., Lichte, A., Burmeister, J., Muhn, P., Jahnke, B., Fesser, D., Erfurth, J., Burgstaller, P. & Klussmann, S. (2002). *Chem. Biol.* **9**, 351–359.

Lorenz, S., Perbandt, M., Lippmann, C., Moore, K., DeLucas, L. J., Betzel, C. & Erdmann, V. A. (2000). *Acta Cryst.* D**56**, 498–500.

Navaza, J. (1994). *Acta Cryst.* A**50**, 157–163.

Nolte, A., Klussmann, S., Bald, R., Erdmann, V. A. & Fürste, J. P. (1996). *Nature Biotechnol.* **14**, 1116–1119.

Otwinowski, Z. & Minor, W. (1997). *Methods Enzymol.* **276**, 307–326.

Perbandt, M., Vallazza, M., Lippmann, C., Betzel, C. & Erdmann, V. A. (2001). *Acta Cryst.* D**57**, 219–224.

Quack, M. (2002). *Angew. Chem. Int. Ed.* **41**, 4618–4630.

Seelig, B. & Jäschke, A. (1999). *Chem. Biol.* **6**, 167–176.

Snell, E. H., Weisberger, S., Helliwell, J. R., Weckert, E., Hölzer, K. & Schroer, K. (1995). *Acta Cryst.* D**51**, 1099–1102.

Sullenger, B. A. & Gilboa, E. (2002). *Nature (London)*, **418**, 252–258.

Tranter, G. E. (1987). *Chem. Phys. Lett.* **135**, 279–281.

Tuerk, C. & Gold, L. (1990). *Science*, **249**, 505–510.

Vallazza, M., Banumathi, S., Perbandt, M., Moore, K., DeLucas, L., Betzel, C. & Erdmann, V. A. (2002). *Acta Cryst.* D**58**, 1700–1703.

Vallazza, M., Senge, A., Lippmann, C., Perbandt, M., Betzel, C. & Erdmann, V. A. (2001). *J. Cryst. Growth*, **232**, 340–352.

Wlotzka, B., Leva, S., Eschgfäller, B., Burmeister, J., Kleinjung, F., Kaduk, C., Muhn, P., Hess-Stump, H. & Klussmann, S. (2002). *Proc. Natl Acad. Sci. USA*, **99**, 8898–8902.